Calorimetric Studies of Bovine Rod Outer Segment Disk Membranes Support a Monomeric Unit for Both Rhodopsin and Opsin

Thomas C. Edrington 5th,* Michael Bennett,[†] and Arlene D. Albert*

*Department of Molecular and Cell Biology, University of Connecticut, Storrs, Connecticut 06250; and [†]Section of Fluorescence Studies, Laboratory of Membrane Biochemistry and Biophysics, National Institute on Alcohol Abuse and Alcoholism, National Institutes of Health, Bethesda, Maryland 20892

ABSTRACT   The photoreceptor rhodopsin is a G-protein coupled receptor that has recently been proposed to exist as a dimer or higher order oligomer, in contrast to the previously described monomer, in retinal rod outer segment disk membranes. Rhodopsin exhibits considerably greater thermal stability than opsin (the bleached form of the receptor), which is reflected in an ∼15°C difference in the thermal denaturation temperatures (T_m) of rhodopsin and opsin as measured by differential scanning calorimetry. Here we use differential scanning calorimetry to investigate the effect of partial bleaching of disk membranes on the T_m of rhodopsin and of opsin in native disk membranes, as well as in cross-linked disk membranes in which rhodopsin dimers are known to be present. The T_ms of rhodopsin and opsin are expected to be perturbed if mixed oligomers are present. The T_m remained constant for rhodopsin and opsin in native disks regardless of the level of bleaching. In contrast, the T_m of cross-linked rhodopsin in disk membranes was dependent on the extent of bleaching. The energy of activation for denaturation of rhodopsin and cross-linked rhodopsin was calculated. Cross-linking rhodopsin significantly decreased the energy of activation. We conclude that in native disk membranes, rhodopsin behaves predominantly as a monomer.

INTRODUCTION

G-protein-coupled receptors (GPCRs) are a large superfamily of cell surface signaling receptors that become activated upon binding a diverse array of natural ligands (for a review, see Pierce et al. (1)). A myriad of diseases including obesity, asthma, heart failure, blindness, depression, and anxiety have been linked to genetic mutations and polymorphisms in GPCRs (2). All GPCRs share the common structural motif of a core bundle of seven transmembrane helices with an extracellular amino-terminal domain and an intracellular carboxyl-terminal domain. For most GPCRs, extracellular ligand binding induces receptor conformational changes that facilitate binding to heterotrimeric guanine nucleotide binding proteins (G-proteins) on the cytoplasmic face of the protein. G-protein binding effectively propagates the extracellular signal culminating in an intracellular response.

It has been proposed that many GPCRs function as homo- and heterodimers within the plasma membrane (3–5). The functional significance of GPCR oligomerization is currently a topic of significant interest in GPCR biology. Although there is evidence that suggests dimerization is necessary for proper functionality and cell surface trafficking of some GPCRs (e.g., the γ-aminobutyruic acid receptor) (for a review, see Prinster et al. (6)), the biological relevance of oligomerization for rhodopsin, the archetypical GPCR, remains a matter of debate (7).

Rhodopsin is a Class A GPCR that shares homologous sequence and structural motifs with 80% of all GPCRs (8).

In the vertebrate retinal rod cell, rhodopsin is responsible for dim light vision. Rhodopsin functions within a densely packed stack of disk shaped membranes encased by the plasma membrane of the rod cell outer segment (ROS) and constitutes >90% of the membrane proteins within the disk membrane (9). Rhodopsin consists of the apo protein opsin with its chromophore ligand, 11-*cis*-retinal, bound. Upon photon absorption, 11-*cis*-retinal isomerizes to all-*trans* retinal causing rhodopsin to undergo conformational changes that result in binding of the heterotrimeric G-protein transducin, thus propagating the biochemical signaling cascade known as phototransduction (for a review, see Baylor (10)).

A wealth of biophysical and biochemical studies, summarized by Chabre and Maire in 2005 (7), established that functional rhodopsin exists as a monomer in native ROS disk membranes. This body of literature has been drawn into question by reports suggesting rhodopsin functions as dimers or even higher order oligomers in native disk membranes (11–13). A molecular model for rhodopsin dimers in native disk membranes has been derived from atomic force microscopy lattice parameters (12,14) (Protein Data Bank ID: 1N3M). This model proposes that rhodopsin dimer formation occurs between transmembrane helix 4 (TM4) and TM5 of adjacent rhodopsin molecules. Cross-linking studies have been used to support the presence of stable rhodopsin dimers in disk membranes (15,16). It was further proposed that transducin binding could be best accommodated by a heterodimer of light-activated opsin and unbleached rhodopsin (17). Although the methods used to establish the dimeric model for functional rhodopsin have been directly challenged (7), the contrasting theory has garnered great

---

attention and as a consequence invigorated investigations into the native oligomeric state of rhodopsin.

In this study, we investigated the potential presence of photoreceptor dimers by exploiting the differences in the temperature of irreversible thermal denaturation (T_m) and the activation energies for thermal denaturation (E_{act}) exhibited by the rhodopsin and opsin forms of this receptor. Rhodopsin and opsin have well separated T_ms. As determined by differential scanning calorimetry (DSC), the T_m is ~72°C for rhodopsin and 55°C for opsin in disk membranes (18,19). Additionally, these two forms of the receptor exhibit distinct E_{act}s, a kinetic parameter determined from the dependence of the T_m on the calorimetric scan rate (20). Both of these parameters are sensitive to alterations of the protein or its membrane environment (20–22). Therefore, the T_m and E_{act} of rhodopsin·opsin heterodimers are expected to be different from homodimers or monomers of either rhodopsin or opsin. Our results show that in partially bleached disk membranes, the T_m and E_{act} of rhodopsin and opsin are independent of the extent of bleaching, that is, independent of the ratio of rhodopsin to opsin. This is consistent with monomers of rhodopsin and of opsin in the disk membrane as shown schematically in Fig. 1 A. Our results further show that when rhodopsin is cross-linked to generate stable dimmers, the thermal denaturation of the dimer species is fundamentally different from that of rhodopsin or opsin in native ROS disk membranes. This is consistent with a dimeric system in which partial bleaching results in some rhodopsin·opsin hetero-
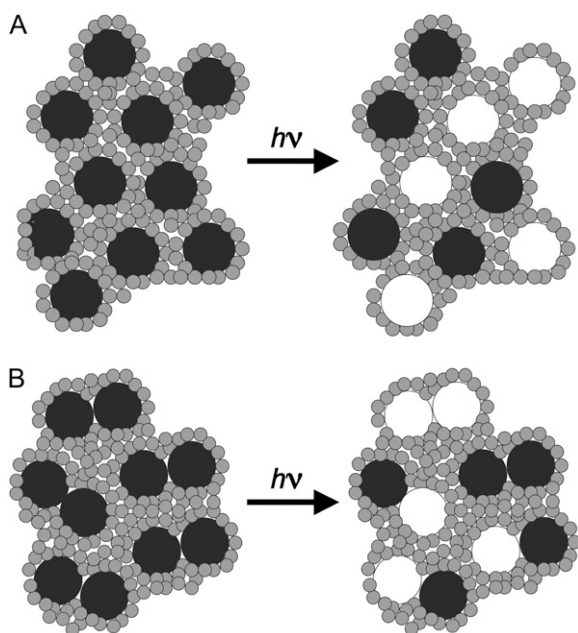
dimers. These two receptor forms affect the stability of each other, altering the T_m and E_{act} of rhodopsin in the heterodimer. These results provide compelling evidence for a monomeric model for rhodopsin in native ROS disk membranes.

MATERIALS AND METHODS

Sample preparation

Frozen bovine retinas were obtained from Lawson (Lincoln, NE). ROS were isolated as described (12). Osmotically intact disk membranes were isolated from retinal ROS by ficoll flotation as described (23). Resulting disk membranes were washed twice in 0.1 M KPO_4^-, pH 7.0, by centrifugation (22,532 × g at r_{avg}; 20 min; 4°C) and resuspended to final rhodopsin concentrations of 1.5–2.0 mg/ml in 10 mM KPO_4^-, pH 7.0. All rhodopsin concentrations were determined from the change in absorbance at 500 nm after photobleaching in the presence of hydroxylamine using an extinction coefficient of 40,000 cm^{-1} M^{-1}. Absorbance spectra were acquired from 265 to 700 nm using a Varian (Palo Alto, CA) Cary 50 UV/VIS spectrophotometer. All samples were prepared under dim red light.

Bleached disk membranes were prepared by exposure to successive flashes of white light from a Sunpak (Tokyo, Japan) auto zoom 333 thyristor flash unit. Spectra of the flashed disk membranes were recorded and the percent bleach was determined from the change in A_{500} relative to the unbleached and fully bleached spectra. Typically, one flash generated a 20–30% bleach (70–80% rhodopsin, 20–30% opsin), and three flashes generated a 50–60% bleach.

Cross-linked rhodopsin samples were prepared immediately after isolation and washing of osmotically intact ROS disk membranes. Disk membranes were resuspended to a final concentration of 0.2 mg/ml of rhodopsin in 0.1 M KPO_4^-, pH 7.0, 150 mM NaCl. The cross-linking reaction was initiated by the addition of dithiobis[succinimidylpropionate] (DSP) in dimethyl sulfoxide from stock solution, such that the final reaction mixture contained no more than 5% dimethyl sulfoxide and was between 0.5 and 2.5 mM DSP. The reaction mixture was incubated on ice for the times indicated. After incubation, the reaction was quenched by the addition of 50 mM glycine from a stock solution of 0.1 M KPO_r^-, pH 7.0, and 1 M glycine. The cross-linked disk membranes were pelleted by centrifugation (22,532 × g at r_{avg}; 20 min; 4°C). Pelleted cross-linked disk membranes were resuspended in 50% sucrose, 0.1 M KPO_r^-, pH 7.0, and centrifuged (82,7000 × g at r_{avg}.; 1 h; 4°C) to remove excess DSP. The resulting floats were washed twice by centrifugation as described above and resuspended in 10 mM KPO_r^-, pH 7.0, to final rhodopsin concentrations between 1.5 and 2.0 mg/ml.

Gel electrophoresis

Samples for SDS-PAGE gel electrophoresis were run on 10% acrylamide gels and silver-stained. Cross-linked and native disk membranes were run in SDS-PAGE sample loading buffer in the absence of β-mercaptoethanol. Cross-linker cleaved samples were cleaved by incubation with 50 mM Tris(2-carboxyethyl)phosphine hydrochloride (TCEP) on ice for 30 min immediately before the addition of sample loading buffer. Samples were kept on ice and were not boiled before loading to avoid temperature-induced aggregation of disk membrane proteins. Gels were imaged and analyzed using a Kodak (Rochester, NY) Gel Logic 100 Imaging System and Kodak 1D Image Analysis Software v3.6. The percent of cross-linked rhodopsin was determined from the percent intensity contribution of the bands corresponding to monomeric and dimeric rhodopsin within a lane. Higher order cross-linking was negligible.

FIGURE 1 Schematic depicting two possible scenarios of rhodopsin (*black circles*) bleached to opsin (*white circles*) in disk membranes. Shaded circles represent the membrane phospholipid headgroups. (*A*) Bleaching monomeric rhodopsin results in independent rhodopsin and opsin monomers. (*B*) Bleaching dimeric rhodopsin results in herterodimers and homodimers of rhodopsin and opsin.

Differential scanning calorimetry

DSC studies were performed on a MicroCal (Northampton, MA) VP-DSC micro calorimeter. Unbleached disk membrane samples were prepared at a rhodopsin concentration of 1.5–2.0 mg/ml. Aliquots were removed and

partially bleached as described above to generate samples containing both rhodopsin and opsin. All samples and buffers were degassed (8 min; 20°C) in a MicroCal Thermovac immediately before loading. Samples were loaded under dim red light. Samples were heated from 20 to 85°C at 0.25, 0.5, 1.0, and 1.5°/min scan rates. At least two consecutive scans were recorded for each sample. The second scan of each native and cross-linked sample was transitionless and was therefore used as a baseline for the initial scan. Analysis of the resulting thermograms was performed using MicroCal Origin 5.0 software. The E_{act} for rhodopsin and cross-linked rhodopsin was determined from the midpoint of the maxima, or T_m, of the endotherms at each scan rate according to the modified Arrhenius expression:

$$\frac{v}{T_m^2} = \frac{AR}{E_{act}} e^{-E_{act}/RT_m},$$

where v is the scan rate, E_{act} is the activation energy, R is the universal gas constant, and A is the Arrhenius frequency factor (24). Further statistical analysis was performed using GraphPad Prism 4 software (GraphPad Software, San Diego, CA).

RESULTS

DSC of native disk membranes

Osmotically intact ROS disk membranes were examined by DSC to determine the affect of increasing concentrations of opsin on the T_m of rhodopsin in native disk membranes. Isolated disk membranes were maintained in dark conditions or were illuminated to bleach up to 55% of the rhodopsin. This generated disk membranes with rhodopsin to opsin ratios of between 1:0 and 1:1. These disk membranes were scanned from 20 to 85°C. Due to the irreversible nature of the thermal denaturation of rhodopsin and opsin, a second consecutive scan of each sample exhibited no transition. This second scan was used to establish the baseline in the resulting thermograms. Thermograms for 0, 22, and 55% bleached disk membranes at a 1.5°/min scan rate are shown in Fig. 2. In agreement with previous studies (18,20), single asymmetric endotherms corresponding to the thermal denaturation of rhodopsin and opsin were observed. The magnitude of each
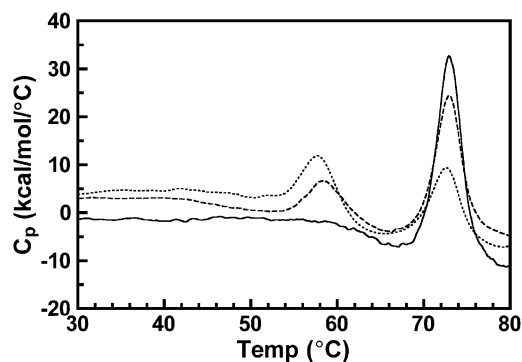
rhodopsin endotherm decreased whereas the magnitude of each opsin endotherm increased proportionally to percent bleach of each sample. Because the T_ms of both rhodopsin and opsin are sensitive to the rate of heating (scan rate), unbleached and partially bleached disk membranes were additionally scanned from 20 to 85°C at 1.0, 0.5, and 0.25°/min scan rates. The T_m of each rhodopsin and opsin endotherm was recorded and plotted as a function of percent bleach for each scan rate (Fig. 3). Linear regression of each data set revealed no statistically significant relationship between the percent bleach and the T_m for either rhodopsin (P values < 0.05) or opsin (P values < 0.10). This is consistent with a previous study using a single scan rate (18). Thus, the T_m of rhodopsin denaturation is independent of the presence of opsin and the T_m of opsin denaturation is independent of the presence of rhodopsin in the membrane.

The denaturation of rhodopsin is a kinetically controlled two-state irreversible process, and the dependence of the rhodopsin T_m on the calorimetric scan rate has been detailed elsewhere (20). Accordingly, the E_{act} for the denaturation of rhodopsin and opsin can be determined from the scan rate dependence of each respective endotherm as described in Materials and Methods (24). In this study, we calculated an E_{act} for rhodopsin denaturation of 165 kcal/mol, in close agreement with our previously determined value of 162 kcal/mol (20) (for representative thermograms of unbleached native disk membranes at 1.5, 1.0, 0.5, and 0.25°/min scan rates, see Fig. 8). The E_{act} for opsin denaturation in native disk membranes in the absence of hydroxylamine was determined to be 131 kcal/mol. As described above, the T_ms of rhodopsin and opsin denaturation are independent of the rhodopsin to opsin ratio. Therefore, by definition, the E_{act} for rhodopsin denaturation must be independent of the presence of opsin and the E_{act} for opsin denaturation must be independent of the presence of rhodopsin.
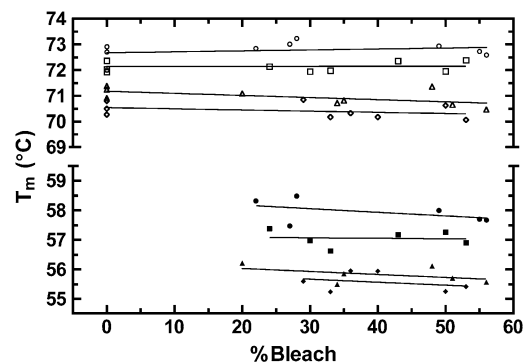

FIGURE 2 Effect of increasing percent bleach on the thermal denaturation of rhodopsin in native disk membranes. Dark-adapted disk membranes in 10 mM KPO_4-, pH 7.0, were exposed to successive flashes of white light to generate 0–55% bleach. Thermograms were acquired from 0 to 85°C at a scan rate of 1.5°/min. Depicted are thermograms of 0% (*solid curve*), 22% (*dashed curve*), and 55% (*dotted curve*) bleached native disk membranes.

FIGURE 3 Dependence of the rhodopsin and opsin temperature of thermal denaturation on bleaching and scan rate. The T_m of each rhodopsin (*open symbols*) and opsin (*solid symbols*) endotherms was recorded from the thermograms of ~0–60% bleached native disk membranes at 1.5 (*circles*), 1.0 (*squares*), 0.5 (*triangles*), and 0.25°/min (*diamonds*) scan rates. Linear regression analysis produced slopes that did not significantly deviate from zero at the 95% (rhodopsin) and 90% (opsin) confidence levels.

DSC of cross-linked disk membranes

Successful chemical cross-linking of rhodopsin in disk membranes and in detergents has been asserted as strong evidence for the existence of rhodopsin dimers in native ROS disk membranes (15,16,25). Therefore, to establish that opsin could influence the T_m of rhodopsin in a dimer, rhodopsin dimers were generated for DSC studies using the same cross-linking technique used in those earlier reports. Purified disk membranes were cross-linked with the cleavable-thiol, primary amine-reactive, homobifunctional N-hydroxysuccimide ester, DSP. Rhodopsin dimers were formed with a concomitant decrease in rhodopsin monomers upon incubation of disk membranes with DSP, consistent with the previous reports (Fig. 4, *lanes 2* and *4*). Higher order oligomers of rhodopsin were not observed in significant quantities. Gel analysis revealed that incubation with 0.5 mM DSP for 2 h or 1.0 mM DSP for 12 h produced 16% and 34% dimeric cross-linked rhodopsin (16X and 34X) relative to monomeric rhodopsin, respectively. Addition of the reducing agent TCEP to the cross-linked disk membranes resulted in the complete loss of dimeric rhodopsin (Fig. 4, *lanes 3* and *5*). This reversibility demonstrated that dimer formation was DSP dependent and not due to nonspecific aggregation; <5% of rhodopsin in noncross-linked disk membranes was dimeric (Fig. 4, *lane 1*). Increasing the DSP concentration to 2.5mM, or increasing the incubation time to 19 h, resulted in no more than 50% dimeric rhodopsin (data not shown).

Thermograms of DSP cross-linked unbleached disk membranes were significantly different from those of native unbleached disk membranes. Fig. 5 depicts representative thermograms of unbleached native and cross-linked disk membranes acquired from 20 to 85°C at a 1.5°/min scan rate. The rhodopsin endotherm broadened and decreased in magnitude with increased cross-linking. Furthermore, cross-linking resulted in the appearance of an exothermic thermal
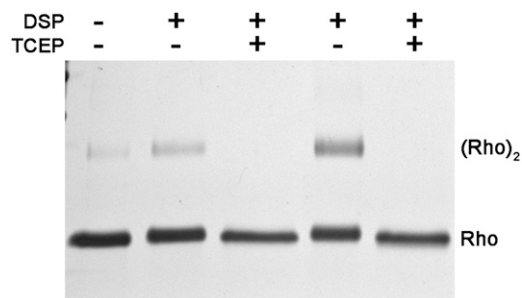

FIGURE 4   SDS-PAGE of native bovine ROS disk membranes (*lane 1*), 16% and 34% dimeric rhodopsin in cross-linked disk membranes (*lanes 2* and *4*, respectively), and cross-linker cleaved disk membranes (*lanes 3* and *5*). The percent dimeric rhodopsin was determined from the relative intensity of the bands corresponding to monomeric and dimeric rhodopsin (*Rho*) in the cross-linked samples. Disk membranes were cross-linked with 0.5 mM DSP for 2 h (*lane 2*) or 1.0 mM DSP for 12 h (*lane 4*). Cross-linked disk membranes were cleaved by incubation with 50 mM TCEP immediately before loading. Quantifiable concentrations of higher order *n*-mers of rhodopsin in the cross-linked samples were not present.
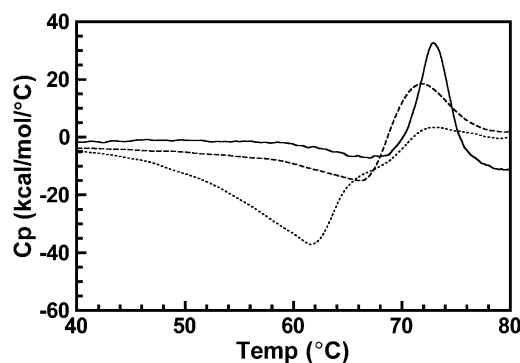
FIGURE 5   Effect of cross-linking on the thermal denaturation of rhodopsin in disk membranes. Representative thermograms of rhodopsin in native disk membranes (*solid curve*), 16% dimeric rhodopsin (*dashed curve*) in cross-linked disk membranes, and 34% dimeric rhodopsin (*dotted curve*) in cross-linked disk membranes were acquired at a scan rate of 1.5°/min.

transition immediately before the rhodopsin endotherm in the unbleached cross-linked samples. The size of the exothermic transition increased and shifted to lower temperatures with increased cross-linking. This type of exothermic transition has been observed for other proteins and is typically attributed to protein aggregation (26–29). To ensure the absence of thermal transitions at temperatures >85°C, cross-linked disk membranes were heated from 20 to 120°C and no additional transitions were observed at >85°C (data not shown).

The thermograms of bleached cross-linked disk membranes were also strikingly different than for bleached native disk membranes. Both 16X and 34X disk membranes were bleached from 0 to 60% and thermograms were acquired as detailed above. After bleaching (Fig. 6), the exothermic transition initially shifted to lower temperatures and decreased in magnitude for both cross-linked samples. However, increasing the percent bleach increased the magnitude of the shifted exothermic transition. As observed with native disk membranes, the rhodopsin endotherm in both cross-linked samples decreased in magnitude with increasing percent bleach. In contrast to native disk membranes, the rhodopsin endotherm became extensively broadened and the T_m decreased in both preparations with increasing percent bleach. Fig. 7 depicts the change in the rhodopsin T_m in 16X and 34X disk membranes from 0 to 60% percent bleach. Linear regression analysis revealed a statistically significant relationship between the change in T_m and percent bleach for both cross-linked samples. The gradient of the resultant slope was proportional to the percentage content of dimeric rhodopsin. The opsin endotherm was not discernable in the thermograms of any cross-linked sample.

To determine the affect of cross-linking on the E_{act} of rhodopsin denaturation, thermograms were acquired of unbleached, cross-linked disk membranes at 1.5, 1.0, 0.5, and 0.25°/min scan rates (Fig. 8). As observed previously, the kinetic dependence of rhodopsin denaturation in native disk membranes resulted in a decreasing rhodopsin T_m as a function of decreasing scan rate. In both cross-linked samples, the
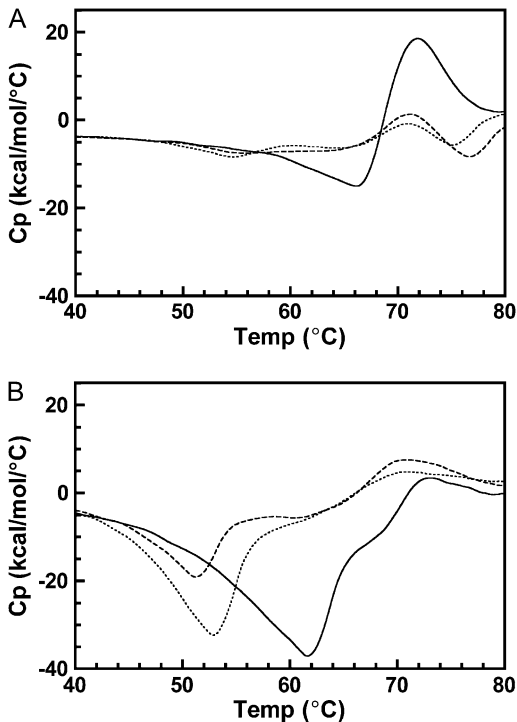
FIGURE 6 Effect of bleaching on the thermal denaturation of cross-linked rhodopsin in disk membranes. Representative thermograms of cross-linked disk membranes at increasing percent bleach. (*A*) 16% dimeric rhodopsin at 0% bleach (*solid curve*), 40% bleach (*dashed curve*), and 57% bleach (*dotted curve*); (*B*) 34% dimeric rhodopsin at 0% bleach (*solid curve*), 28% bleach (*dashed curve*), and 60% bleach (*dotted curve*). Thermograms of cross-linked disk membranes were acquired at a 1.5°/min scan rate and smoothed over 25 points using Origin 5.0 software for clarity.

dependence of the rhodopsin T_m on the scan rate was greater than that of rhodopsin in native disk membranes. The observed E_{act} for 16X and 34X rhodopsin of 109 kcal/mol and 77 kcal/mol, respectively, shows that the E_{act} decreased proportionally to the increase of dimeric rhodopsin. In each of the cross-linked rhodopsin samples, the exothermic transition exhibited a significant dependence on the scan rate. The E_{act} for the exothermic transitions in both 16X and 34X cross-linked samples was determined to be 23 kcal/mol and 15 kcal/mol, respectively (Fig. 8, *E* and *F*). Previous DSC studies of bovine insulin reported a similar scan rate dependence of insulin aggregation (26). Interestingly, the dependence of the exothermic transition on the calorimetric scan rate increased with increasing percentage of cross-linking.

DISCUSSION

The recently renewed interest in rhodopsin dimerization and its association into high order arrays was stimulated by atomic force microscopy images of rows of rhodopsin dimers arranged in paracrystalline arrays in the plane of the disk membrane (30). These images were further supported by cross-linking studies that purported to trap preexisting dimers of rhodopsin (15). These data suggested rhodopsin forms
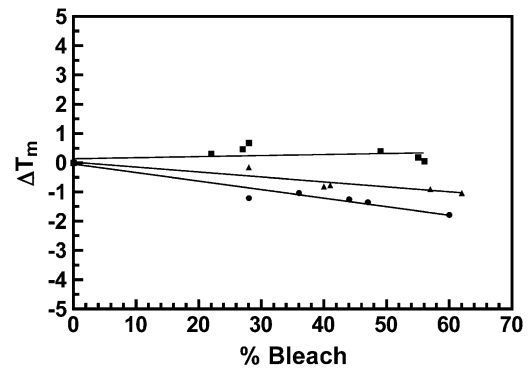

FIGURE 7 Change in T_m as a function of percent bleach for rhodopsin in native disk membranes (*squares*), 16% dimeric rhodopsin in cross-linked disk membranes (*triangles*), and 34% dimeric rhodopsin in cross-linked disk membranes (*circles*). The change in T_m was calculated relative to the average T_m of at least three scans of unbleached disk membranes ($T_{mavg} = 72.5 \pm 0.5$, 71.8 ± 0.1, and 72.9 ± 0.3, respectively). Differences in the T_{mavg} represent variability between disk membrane and cross-linking preparations. The T_m of each respective endotherm was recorded from excess heat capacity curves of ~0–60% bleached disk membranes at a 1.5°/min scan rate. Linear regression analysis produced slopes that significantly deviated from zero for the cross-linked disk membranes (>99.9% confidence level).

stable dimers in native disks, which then further associate to generate higher order species. If rhodopsin forms stable dimers, it is reasonable to propose that under partial bleach conditions, some heterodimers consisting of both rhodopsin and opsin would exist (see Fig. 1). Indeed, heterodimers have been proposed as the functional receptor unit to accommodate the binding of the large G-protein, transducin (17). Because bleaching of a single rhodopsin is sufficient to activate the visual cascade, this dimer model requires that opsin and rhodopsin coexist in the same dimer. Here we have tested this hypothesis by investigating the calorimetric melting transitions of rhodopsin and opsin in ROS disk membranes.

Previous DSC studies have shown the T_m and E_{act} of the receptor to be exquisitely sensitive to a spectrum of perturbations to the protein and to its surrounding membrane environment. The most dramatic of these is the bleaching event itself. The decrease in both the thermal denaturation temperature (31) and the activation energy of denaturation (20) when rhodopsin is bleached to opsin demonstrates the role of the chromophore, 11-*cis* retinal, in the thermal stability of the photoreceptor. The T_m of rhodopsin and opsin is also remarkably sensitive to changes in the composition of the surrounding lipid bilayer. The T_m increases when the membrane is made more ordered by increasing the content of cholesterol (22) or by increasing the saturation of the lipid bilayer (21). Proteolytic cleavage of the cyotoplasmic loops or of the carboxyl terminus of the receptor decreases the T_m (20). Clearly, alterations of either the protein integrity or of its environment affect the T_m of rhodopsin thermal denaturation. In the DSC experiments described herein, as the temperature is increased from 20 to 85°C, any opsin that is present in the disk membrane will denature before rhodopsin due to the
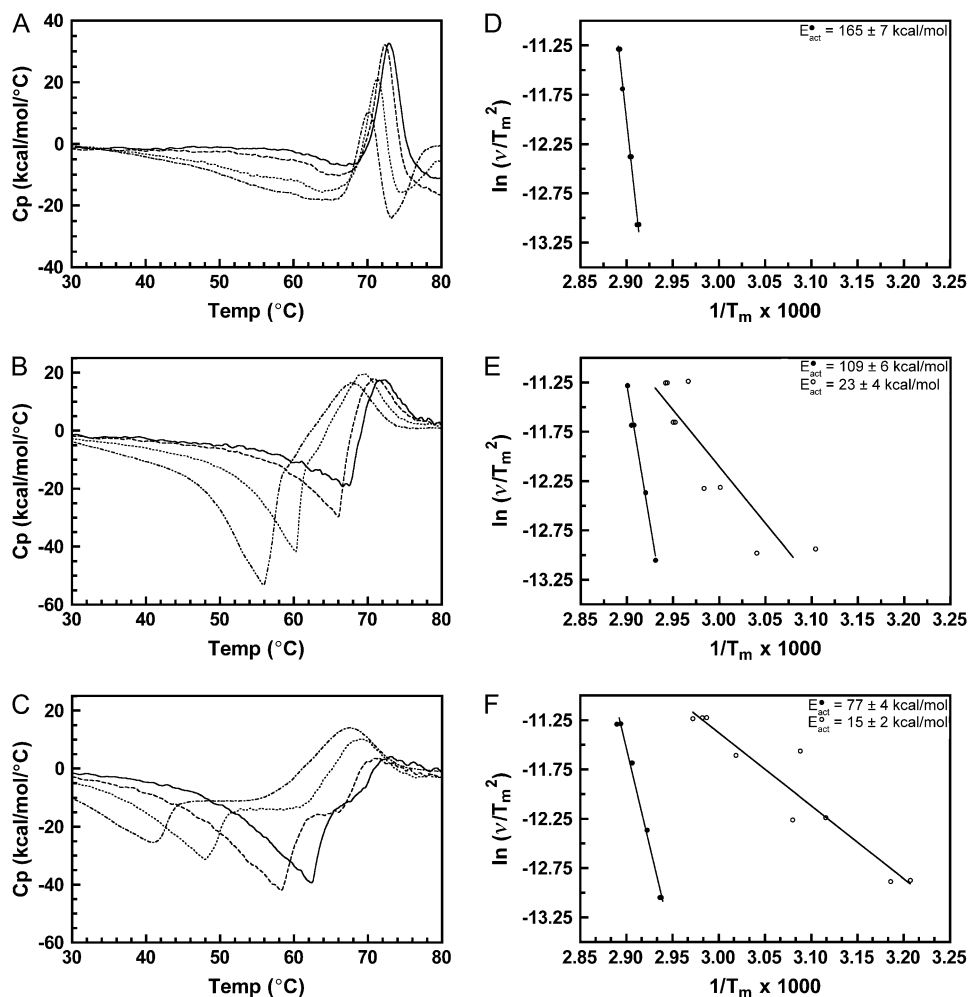
FIGURE 8 Determination of the E_{act} of denaturation for native and cross-linked rhodopsin in disk membranes. Representative thermograms and plots of $\ln(v/T_m^2)$ versus $1/T_m$ for (A and D) unbleached native disk membranes, (B and E) 16% dimeric rhodopsin in cross-linked disk membranes, and (C and F) 34% dimeric rhodopsin in cross-linked disk membranes. The thermograms were acquired at scan rates of 1.5°/min (solid curves), 1.0°/min (dashed curves), 0.5°/min (dotted curves), and 0.25°/min (dashed-dot-dashed curves). The scan rates and T_ms of each endothermic (solid circles) and exothermic (open circles, for the cross-linked samples only) transition were used for the modified Arrhenius plots. At least two T_m values for each transition were used. The E_{act}s for the transitions were determined from the slope of each $\ln(v/T_m^2)$ versus $1/T_m$ plot according to the equation $\ln(v/T_m^2) = $ const. $- E_{act}/R(1/T_m)$ (20,24) (see Materials and Methods). Lines are best fit as determined by linear regression.

~15°C difference in their T_ms. If stable rhodopsin·opsin heterodimers are present, then upon heating, the denaturation of opsin will have a direct impact on the protein-protein interactions at the heterodimer interface. Because the T_m of rhodopsin is dependent on the state and the environment of the protein, the T_m of rhodopsin in rhodopsin·opsin heterodimers would be influenced by the decreased thermal stability of its opsin dimer partner. Conversely, the T_m of opsin in the corresponding heterodimer would be analogously influenced by the increased thermal stability of its rhodopsin dimer partner. In this scenario, the thermal denaturation of the rhodopsin·opsin heterodimer would display distinctly different characteristics than that of rhodopsin and opsin monomers or homodimers.

In this DSC study, the T_m of rhodopsin and opsin thermal denaturation in native disk membranes was characterized as a function of the percent of bleached pigment (percent opsin). The maximum percent bleach was slightly >50%, which generated a rhodopsin/opsin ratio of ~1:1. This is sufficient to expect substantial formation of rhodopsin-opsin dimers. Thermograms were obtained at four different scan rates (1.5, 1.0, 0.5, and 0.25°/min) because the thermal denaturation of rhodopsin is a kinetic process and thus the T_m is sensitive to scan rate. Any affect on the T_m would be amplified at slower

scan rates due to this kinetic dependence. In native disk membranes, the T_m of neither rhodopsin nor opsin could be correlated to the percent bleach regardless of the scan rate used. Therefore, the temperature of thermal denaturation for both rhodopsin and opsin is independent of the relative levels of each of these species in the native disk membrane. This suggests that they are isolated from each other in the plane of the disk membrane. These data are most readily explained by the monomeric model for rhodopsin and opsin in the disk membrane. Furthermore, this invariance of T_m with percent bleach is consistent with the independence of E_{act} with respect to the rhodopsin/opsin ratio.

Chemical cross-linking of native disk membranes, which has been shown to produce rhodopsin dimers and as well as small amounts of higher order rhodopsin oligomers (15, 16,25,32), was used to investigate the thermal behavior of stable rhodopsin dimers. Cross-linked rhodopsin dimers do not represent a truly native dimeric species in that they cannot be in equilibrium with monomeric rhodopsin due to covalent association via the chemical cross-linker. However, chemical cross-linking of rhodopsin to induce rhodopsin dimers can provide a model to examine a stable dimeric rhodopsin species. Earlier rhodopsin cross-linking studies that utilized

glutaraldehyde cross-linking attributed the formation of rhodopsin oligomers to random collisions between rapidly diffusing monomeric rhodopsin molecules in the disk membrane (32). More recent studies that used the cross-linking reagent DSP interpreted the formation of rhodopsin dimers upon cross-linking as the trapping of a preexisting rhodopsin dimeric state (15). Our cross-linking results using DSP are in good agreement with both of these studies in that the primary cross-linked species is dimeric. Also, as the case in these previous studies, the majority of rhodopsin in native disk membranes could not be cross-linked and remained monomeric.

The thermal behavior of rhodopsin was investigated in disks in which ~16% and 34% of the rhodopsin was cross-linked using DSP to form stable dimers. Even at these levels of cross-linking, DSC thermograms of cross-linked disk membranes displayed dramatically different characteristics from thermograms of native disk membranes in two important ways. First, the endothermic peak corresponding to rhodopsin was substantially broadened relative to that observed for native disks. It is likely that this peak represents the thermal transition of both cross-linked dimeric and monomeric rhodopsin. Second, in contrast to the native disks, there was a striking exothermic transition typical of a protein aggregation event before the rhodopsin endotherm that was dependent on both the extent of cross-linking and the scan rate. The simplest interpretation of the decreased E_{act} for this transition with increased percent cross-linking is that cross-linking of rhodopsin likely reduces the energetic barrier associated with two molecules of rhodopsin coming into close apposition within the lipid bilayer. Therefore, it is possible that the cross-linking of rhodopsin nucleates aggregation.

In contrast to the studies in native disks, the apparent T_m of rhodopsin in cross-linked disk membranes was not independent of the presence of opsin. Disk membranes with 16% and 34% cross-linked dimeric rhodopsin exhibited apparent rhodopsin T_ms with a statistically significant correlation to the percent bleach. The E_{act} for denaturation of rhodopsin in cross-linked disk membranes decreased relative to rhodopsin in native disk membranes. Finally, the dependence of the rhodopsin T_m on the percent bleach and the observed decrease in the energy of activation for cross-linked disk membranes were proportional to the relative percent dimeric rhodopsin. These results support our hypothesis in that increasing concentrations of opsin affect the T_m of rhodopsin in disk membranes containing homo- and heterodimeric rhodopsin and opsin. Furthermore, our observations that it requires only a minor extent of rhodopsin cross-linking to significantly alter the kinetics of unfolding and promote aggregation of this receptor highlights the sensitivity of the protein to manipulation.

It is interesting to compare the DSC scans of bacteriorhodopsin in its native membrane to those of rhodopsin in disk membranes. In the purple membrane, bacteriorhodopsin exists as trimers, which are further organized into a paracrystalline array. Thermograms of bacteriorhodopsin exhibit a melting transition before the main transition (33,34). This pretransition has been interpreted as resulting from the reordering of the crystalline array and likely involves the dissociation of the trimer unit. The thermograms of rhodopsin in native disk membranes reported here are somewhat asymmetric due to the kinetic nature of its thermal denaturation. However, they are very well defined with no indication of a pretransition or a shoulder for either the rhodopsin or opsin species. This is in contrast to the more complex thermograms acquired of disk membranes in which stable dimers have been generated by chemical cross-linking.

Among the challenges of determining the monomeric versus oligomeric state of rhodopsin is differentiating physiologically important protein-protein associations from those that are a product of experimental conditions or random association. Rhodopsin is densely packed in the plane of the disk membrane. The disk membrane has a lipid/protein ratio of ~75:1 and a single rhodopsin monomer requires ~30 phospholipids to form a tight annulus of protein-associated phospholipids (35). Therefore, on average, rhodopsin molecules are typically separated by ~2–3 phospholipids and random protein-protein associations must be considered as a source of dimerization.

Another challenge of integral membrane protein investigations is the understanding of the complex hydrophobic environment in which membrane proteins reside. This is a potential problem in studies using detergents or reconstituted membranes. Hydrophobic mismatch, which is defined as the difference in length between the hydrophobic transmembrane region of integral membrane proteins and the equilibrium thickness of the membrane bilayer, has recently been implicated in rhodopsin oligomer formation (36). Furthermore, molecular dynamic simulations predicted a self-assembly of rhodopsin monomers that was dependent on the hydrophobic mismatch of rhodopsin and the bilayer acyl chains (37). Rhodopsin oligomerization observed in reconstituted or in detergent solubilized systems should be interpreted with caution given its sensitivity to the surrounding bilayer environment. Even with extensive dialysis, some detergent remains in reconstituted membranes. It is for this reason we restricted our studies to native disk membranes. In these studies, rhodopsin properties were not complicated by the presence of detergent or of non-native lipids.

The functional significance of rhodopsin oligomerization remains to be shown. It has been proposed that transducin is too large to appropriately bind a rhodopsin monomer and that a dimer provides the required surface for transducin binding (17). However, recent studies of rhodopsin monomers isolated in reconstituted high density lipoproteins and nanoscale lipid bilayers have shown that the monomer is fully capable of transducin activation (38,39). Additionally, docking simulations reveal that the optimal stoichiometric ratio for rhodopsin/transducin binding is 1:1 (40). Together with the results presented here, these observations support our previously proposed model for transducin activation, in which the energy of substrate binding to monomeric-activated rhodopsin drives

a conformational change in heterotrimeric transducin ($G_{t\alpha\beta\gamma}$). This conformational trigger leads to guanosine diphosphate-guanosine triphosphate exchange and dissociation of the $G_{t\alpha}$ and $G_{t\beta\gamma}$ transducin subunits (41).

REFERENCES

1. Pierce, K. L., R. T. Premont, and R. J. Lefkowitz. 2002. Seven-transmembrane receptors. *Nat. Rev. Mol. Cell Biol.* 3:639–650.

2. Insel, P. A., C. M. Tang, I. Hahntow, and M. C. Michel. 2007. Impact of GPCRs in clinical medicine: monogenic diseases, genetic variants and drug targets. *Biochim. Biophys. Acta.* 1768:994–1005.

3. Javitch, J. A. 2004. The ants go marching two by two: oligomeric structure of G-protein-coupled receptors. *Mol. Pharmacol.* 66:1077–1082.

4. Terrillon, S., and M. Bouvier. 2004. Roles of G-protein-coupled receptor dimerization. *EMBO Rep.* 5:30–34.

5. Park, P. S., S. Filipek, J. W. Wells, and K. Palczewski. 2004. Oligomerization of G protein-coupled receptors: past, present, and future. *Biochemistry.* 43:15643–15656.

6. Prinster, S. C., C. Hague, and R. A. Hall. 2005. Heterodimerization of G protein-coupled receptors: specificity and functional significance. *Pharmacol. Rev.* 57:289–298.

7. Chabre, M., and M. le Maire. 2005. Monomeric G-protein-coupled receptor as a functional unit. *Biochemistry.* 44:9395–9403.

8. Davies, M. N., D. E. Gloriam, A. Secker, A. A. Freitas, J. Timmis, and D. R. Flower. 2007. Proteomic applications of automated GPCR classification. *Proteomics.* 7:2800–2814.

9. Papermaster, D. S., and W. J. Dreyer. 1974. Rhodopsin content in the outer segment membranes of bovine and frog retinal rods. *Biochemistry.* 13:2438–2444.

10. Baylor, D. 1996. How photons start vision. *Proc. Natl. Acad. Sci. USA.* 93:560–565.

11. Palczewski, K. 2006. G protein-coupled receptor rhodopsin. *Annu. Rev. Biochem.* 75:743–767.

12. Fotiadis, D., B. Jastrzebska, A. Philippsen, D. J. Muller, K. Palczewski, and A. Engel. 2006. Structure of the rhodopsin dimer: a working model for G-protein-coupled receptors. *Curr. Opin. Struct. Biol.* 16:252–259.

13. Ridge, K. D., and K. Palczewski. 2007. Visual rhodopsin sees the light: structure and mechanism of G protein signaling. *J. Biol. Chem.* 282:9297–9301.

14. Liang, Y., D. Fotiadis, S. Filipek, D. A. Saperstein, K. Palczewski, and A. Engel. 2003. Organization of the G protein-coupled receptors rhodopsin and opsin in native membranes. *J. Biol. Chem.* 278:21655–21662.

15. Suda, K., S. Filipek, K. Palczewski, A. Engel, and D. Fotiadis. 2004. The supramolecular structure of the GPCR rhodopsin in solution and native disc membranes. *Mol. Membr. Biol.* 21:435–446.

16. Jastrzebska, B., T. Maeda, L. Zhu, D. Fotiadis, S. Filipek, A. Engel, R. E. Stenkamp, and K. Palczewski. 2004. Functional characterization of rhodopsin monomers and dimers in detergents. *J. Biol. Chem.* 279:54663–54675.

17. Filipek, S., K. A. Krzysko, D. Fotiadis, Y. Liang, D. A. Saperstein, A. Engel, and K. Palczewski. 2004. A concept for G protein activation by G protein-coupled receptor dimers: the transducin/rhodopsin interface. *Photochem. Photobiol. Sci.* 3:628–638.

18. Khan, S. M., W. Bolen, P. A. Hargrave, M. M. Santoro, and J. H. McDowell. 1991. Differential scanning calorimetry of bovine rhodopsin in rod-outer-segment disk membranes. *Eur. J. Biochem.* 200:53–59.

19. Shnyrov, V. L., and A. L. Berman. 1988. Calorimetric study of thermal denaturation of vertebrate visual pigments. *Biomed. Biochim. Acta.* 47:355–362.

20. Landin, J. S., M. Katragadda, and A. D. Albert. 2001. Thermal destabilization of rhodopsin and opsin by proteolytic cleavage in bovine rod outer segment disk membranes. *Biochemistry.* 40:11176–11183.

21. Polozova, A., and B. J. Litman. 2000. Cholesterol dependent recruitment of di22:6-PC by a G-protein-coupled receptor into lateral domains. *Biophys. J.* 79:2632–2643.

22. Albert, A. D., K. Boesze-Battaglia, Z. Paw, A. Watts, and R. M. Epand. 1996. Effect of cholesterol on rhodopsin stability in disk membranes. *Biochim. Biophys. Acta.* 1297:77–82.

23. Smith, H. G., Jr., G. W. Stubbs, and B. J. Litman. 1975. The isolation and purification of osmotically intact discs from retinal rod outer segments. *Exp. Eye Res.* 20:211–217.

24. Sanchez-Ruiz, J. M., J. L. Lopez-Lacomba, M. Cortijo, and P. L. Mateo. 1988. Differential scanning calorimetry of the irreversible thermal denaturation of thermolysin. *Biochemistry.* 27:1648–1652.

25. Medina, R., D. Perdomo, and J. Bubis. 2004. The hydrodynamic properties of dark- and light-activated states of *n*-dodecyl beta-D-maltoside-solubilized bovine rhodopsin support the dimeric structure of both conformations. *J. Biol. Chem.* 279:39565–39573.

26. Dzwolak, W., R. Ravindra, J. Lendermann, and R. Winter. 2003. Aggregation of bovine insulin probed by DSC/PPC calorimetry and FTIR spectroscopy. *Biochemistry.* 42:11347–11355.

27. van Teeffelen, A. M., M. B. Meinders, and H. H. de Jongh. 2005. Identification of pitfalls in the analysis of heat capacity changes of beta-lactoglobulin A. *Int. J. Biol. Macromol.* 37:28–34.

28. Rochu, D., N. Beaufet, F. Renault, N. Viguie, and P. Masson. 2002. The wild type bacterial Co(2+)/Co(2+)-phosphotriesterase shows a middle-range thermostability. *Biochim. Biophys. Acta.* 1594:207–218.

29. Lohner, K., and A. F. Esser. 1991. Thermal unfolding and aggregation of human complement protein C9: a differential scanning calorimetry study. *Biochemistry.* 30:6620–6625.

30. Fotiadis, D., Y. Liang, S. Filipek, D. A. Saperstein, A. Engel, and K. Palczewski. 2003. Atomic-force microscopy: rhodopsin dimers in native disc membranes. *Nature.* 421:127–128.

31. Miljanich, G. P., M. F. Brown, S. Mabrey-Gaud, E. A. Dratz, and J. M. Sturtevant. 1985. Thermotropic behavior of retinal rod membranes and dispersions of extracted phospholipids. *J. Membr. Biol.* 85:79–86.

32. Downer, N. W. 1985. Cross-linking of dark-adapted frog photoreceptor disk membranes. Evidence for monomeric rhodopsin. *Biophys. J.* 47:285–293.

33. Shnyrov, V. L., and P. L. Mateo. 1993. Thermal transitions in the purple membrane from *Halobacterium halobium*. *FEBS Lett.* 324:237–240.

34. Jackson, M. B., and J. M. Sturtevant. 1978. Phase transitions of the purple membranes *of Halobacterium halobium*. *Biochemistry.* 17:911–915.

35. Stubbs, G. W., and B. J. Litman. 1978. Effect of alterations in the amphipathic microenvironment on the conformational stability of bovine opsin. 1. Mechanism of solubilization of disk membranes by the nonionic detergent, octyl glucoside. *Biochemistry.* 17:215–219.

36. Botelho, A. V., T. Huber, T. P. Sakmar, and M. F. Brown. 2006. Curvature and hydrophobic forces drive oligomerization and modulate activity of rhodopsin in membranes. *Biophys. J.* 91:4464–4477.

37. Periole, X., T. Huber, S. J. Marrink, and T. P. Sakmar. 2007. G protein-coupled receptors self-assemble in dynamics simulations of model bilayers. *J. Am. Chem. Soc.* 129:10126–10132.

38. Bayburt, T. H., A. J. Leitz, G. Xie, D. D. Oprian, and S. G. Sligar. 2007. Transducin activation by nanoscale lipid bilayers containing one and two rhodopsins. *J. Biol. Chem.* 282:14875–14881.

39. Whorton, M. R., M. P. Bokoch, S. G. Rasmussen, B. Huang, R. N. Zare, B. Kobilka, and R. K. Sunahara. 2007. A monomeric G protein-coupled receptor isolated in a high-density lipoprotein particle efficiently activates its G protein. *Proc. Natl. Acad. Sci. USA.* 104:7682–7687.

40. Dell'Orco, D., M. Seeber, and F. Fanelli. 2007. Monomeric dark rhodopsin holds the molecular determinants for transducin recognition: insights from computational analysis. *FEBS Lett.* 581:944–948.

41. Yeagle, P. L., and A. D. Albert. 2003. A conformational trigger for activation of a G protein by a G protein-coupled receptor. *Biochemistry.* 42:1365–1368.